

METEOROLOGICAL SATELLITE INFRARED VIEWS OF CLOUD GROWTH ASSOCIATED WITH THE DEVELOPMENT OF SECONDARY CYCLONES

WILLIAM E. SHENK

Goddard Space Flight Center, NASA, Greenbelt, Md.

ABSTRACT

During March 1962, the cloud changes associated with the predevelopment and development periods of two secondary cyclones in the North Pacific Ocean were viewed on at least two successive days by the 8–12 μ "window" channel of the TIROS IV meteorological satellite. Both secondary cyclones developed at the base of the occlusion. For the two cases, when the secondary circulations were first noticeable on the surface chart, the equivalent blackbody temperatures (T_{BB}) as measured by the radiometer averaged 15°K colder than the day before in the northeast quadrant relative to the base of the occlusion. The average T_{BB} was taken over an area of approximately 300,000 mi². For two other cases, an average warming of 4°K occurred from day to day over the same area relative to the base of the occlusion when no significant secondary development occurred and when the primary occluded cyclone was slowly weakening. These results suggest that, with the assistance of meteorological satellite radiation data, considerable cloud growth is noticeable prior to the generation of a secondary cyclone at the base of the occlusion.

1. INTRODUCTION

A secondary extratropical cyclone is a cyclone that forms near, or in association with, a primary cyclone. Often, the secondary cyclone intensifies and deepens sufficiently to absorb the circulation of the primary cyclone, thus becoming the only remaining circulation. There seem to be two preferred areas of development relative to the primary cyclone: one area at the base of the occlusion, the other southwest of the base of the occlusion along the trailing cold front. From either of these preferred locations, development often proceeds rapidly. Thus, it is important that the presence of these new circulations be determined quickly. Early detection is especially difficult over oceans where conventional meteorological data are sparse.

The East Coast of the United States is a preferred area for secondary development. This usually occurs along (or just off) the coastline during the late fall, winter, and early spring period from the Carolinas to New Jersey while the primary cyclone is advancing across the Great Lakes. Early warning of the secondary development is often provided by rapidly falling barometric pressures east of the Appalachian Mountains and swift advance of the precipitation shield and/or intensification of precipitation over the same region. The behavior of the precipitation patterns suggests that changes might be noted in the cloud deck that would indicate secondary development at an earlier stage. Substantial changes in the areal extent and/or vertical development of clouds near the region of secondary development would be anticipated prior to, or coincident with, the evidence of a surface circulation. Cloud changes noted during the early stages of U.S. East Coast secondary developments are assumed to be similar for secondary developments over oceanic areas. Over land areas, where conventional meteorological data are plentiful (such as the U.S. East Coast), surface observations provide information on the clouds from below. Meteorological satellites can provide cloudiness information from above, while cloud base and cloud top heights can frequently be

calculated from radiosonde measurements. Additionally, such information is supplied by the numerous aircraft flying in the eastern half of the United States. Over the oceans, the only sensors capable of providing detailed cloud information over large areas are carried on board meteorological satellites. The purpose of this paper is to determine what three-dimensional cloud changes occur with the development of secondary cyclones over oceanic regions as seen by meteorological satellites.

BACKGROUND

Past research has shown that striking cloud formations observed by satellites are indicative of the presence of a secondary cyclone. Using the vidicon data from TIROS IX, Anderson et al. (1966) showed evidence of a secondary development in the Pacific by noting two cyclonic cloud spirals that were close together. One spiral was associated with an old occluded cyclone, and the other with a new wave that had developed on a front to the southeast of the occluded storm. The double cloud spiral is anomalous to the classic cloud pattern associated with a simple occluded system (Boucher et al. 1963).

Another case of secondary storm development as seen by a satellite has been documented by Sherr and Rogers (1965). This system was spawned along the trailing cold front some 14° south of the old occluded primary cyclone. A pronounced widening of the frontal cloud band was noticeable both in the TIROS IV vidicon pictures and in the patterns of equivalent blackbody temperatures from the window radiation channel of a five-channel scanning medium resolution radiometer carried on board the same satellite. The window radiation measurements also showed that a sizable area of relatively low equivalent blackbody temperatures indicating relatively high cloud tops was located just west and north of the surface position of the secondary cyclone, and this area was detached from the higher clouds farther north near the primary storm center. This particular secondary cyclone, which was only a weak

wave when the pronounced bulging was observed, intensified rapidly and became the main storm within 24 hr.

The above discussion indicates that, by the time a surface secondary wave has developed along a trailing cold front, substantial three-dimensional cloud growth has occurred along the frontal cloud band. It is still not clear when this cloud growth commences relative to the time when the secondary cyclone can be detected by conventional data. The substantial three-dimensional cloud growth noted by Sherr and Rogers (1965) in the development of the Pacific secondary cyclone suggests that large changes in the clouds may precede secondary surface development.

CASE SELECTION

For studying the three-dimensional cloud changes associated with secondary storm development, radiation data are needed over a substantial portion of the eastern semicircle of the primary storm circulation for at least 2 consecutive days. A suitable period that met the above criteria encompassed selected dates in March 1962 when two secondaries developed near the base of the occlusion that extended south and east of the primary cyclone center in the North Pacific Ocean. The window radiation data were provided by the five-channel medium resolution radiometer on board the TIROS IV meteorological satellite. Also, two cases were selected during the same month and year when little or no secondary development was noticeable. The cloud changes were observed during the gradual weakening process of the occlusion associated with the primary cyclone and compared with the cloud changes noted with secondary development.

Table 1 is a summary of the dates, times, and orbit numbers for each case. The satellite coverage was at night; thus, there were no concurrent vidicon data.

2. THE FIVE-CHANNEL SCANNING MEDIUM RESOLUTION RADIOMETER EXPERIMENT

The TIROS IV meteorological satellite was injected into an orbit with an apogee of 845 km, perigee of 710 km, period of 100.4 min, and inclination of 48.30°. Other detailed information on the spacecraft can be found in the *TIROS IV Radiation Data Catalog and Users' Manual* (Goddard Space Flight Center 1963).

The TIROS IV five-channel medium resolution scanning radiometer was mounted in the satellite such that the optical axes were inclined 45° to the satellite spin axis. The viewing directions were designated as "floor" or "wall" according to their orientation in the satellite. Two of the channels responded to emitted terrestrial radiation from the earth and its atmosphere, two more channels sensed reflected solar radiation, and the fifth channel was used to transmit a redundant time reference signal. At a satellite altitude of about 780 km, the resolution of the radiometer was about 68 km at nadir.

One channel sensed terrestrial radiation in the 8–12 μ atmospheric window. The upwelling radiation was received

TABLE 1.—Summary of TIROS IV radiation data used for each case

Case no.	Date (March 1962)	Approximate time (GMT)	Orbit no.
1	3	1200	329, 330
	4	1200	344, 345
	5	1100	358, 359
2	16	1000	514, 515, 516
	17	0900	528, 529, 530
3	19	1000	558
	20	0900	572
	21	0900	586
4	21	0700	585
	22	0400	598

in this spectral region primarily from the earth's surface and/or clouds. A minor contribution to the total sensed radiance comes from atmospheric constituents—principally water vapor and ozone. Since this study was concerned with radiance changes from day to day, precise knowledge of the absolute measurement was not necessary. Therefore, the ozone and water vapor contributions to the total radiance were ignored. Also, no corrections were applied for a slow degradation of the radiometer or for errors (about 1° latitude) in the geographic positioning of the radiometric data. A more complete discussion is given by Shenk (1970) of the degradation and geographic positioning problems associated with the TIROS IV radiation data.

A convenient method of displaying the radiometric data is on a grid print map. At each grid point, the digitized equivalent blackbody temperatures closest to the geographical location of the grid point are averaged, and this average is printed. A Mercator map projection with a 1:10,000,000 map scale was used in this study. The spacing of the grid points (called the mesh interval) was 1.25° of longitude for this scale.

3. SUMMARY OF THE CASES

Grid print maps of the window radiation data were prepared at approximately 24-hr intervals. Individual maps were prepared for each orbit instead of compositing the data for a series of orbits on one map when it became necessary to use data from more than one orbit for maximum coverage of a cyclone. The data along the edges of orbits adjacent to the one which gave the primary coverage of a cyclone were then shifted slightly to fit the data along the edges of the primary coverage orbit. Movement of the clouds in one TIROS orbital period probably causes most of the shift in the radiation patterns (some of the shift could be caused by attitude differences between orbits).

Figures 1–3 depict the window radiation patterns for March 3, 4, and 5, respectively. In these and all of the remaining figures showing radiation measurements, the dashed lines indicate radiation data spliced from orbits

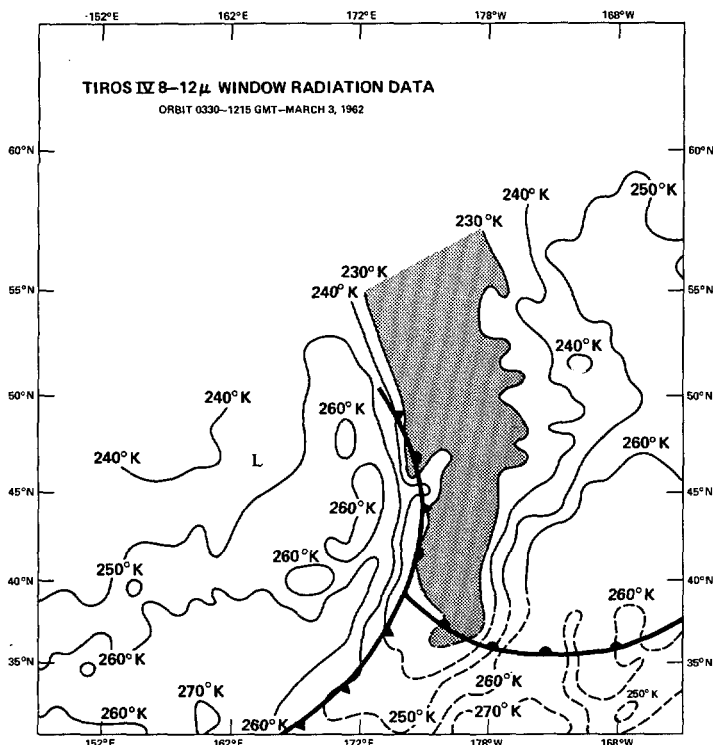


FIGURE 1.—TIROS IV window radiation data for Mar. 3, 1962 (orbit 330); dashed lines show data added from orbit 329.

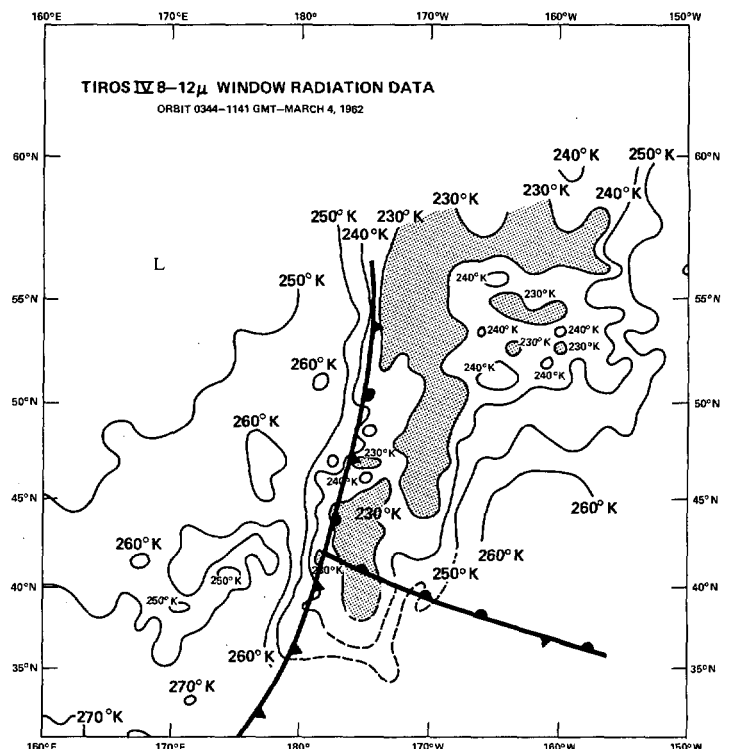


FIGURE 2.—TIROS IV window radiation data for Mar. 4, 1962 (orbit 344); dashed lines show data added from orbit 343.

adjacent to the primary coverage orbit. Frontal positions were determined from synoptic charts prepared by the National Meteorological Center (NMC). Some adjustment was occasionally made in the frontal position to fit the cloud patterns, without violating conventional surface observations. The eastern Pacific case was one in which a very weak wave developed on the front of the south-southeast of the primary cyclone. This wave, shown as a dashed L in figure 3, rippled rapidly up the front as a stable wave and filled within 24 hr. There was never evidence of a complete circulation on any surface map during the short history of the system. Gradual weakening of the occlusion occurred during the 3-day period and is reflected in the changes in the radiation field. The coverage of equivalent blackbody temperatures below 230°K was quite extensive on March 3 and only spotty on March 5 while the size of the frontal band changed slightly. Figures 4–6 show the surface charts for 1200 GMT for the same 3 days. These figures illustrate the steady weakening and filling of the large primary cyclone and the position and strength of the minor wave mentioned above. A 500-mb broad trough was present in the region for the same period. On the last day (March 5), the 500-mb broad stream was perturbed by a weak shortwave trough which probably contributed to the formation of the weak wave at 42° N., 170° W. (fig. 6). The trend of increased equivalent blackbody temperatures was also noted in the region immediately to the east and northeast of the base of the occlusion for the remaining case where no secondary cyclone development occurred, reflecting the gradual

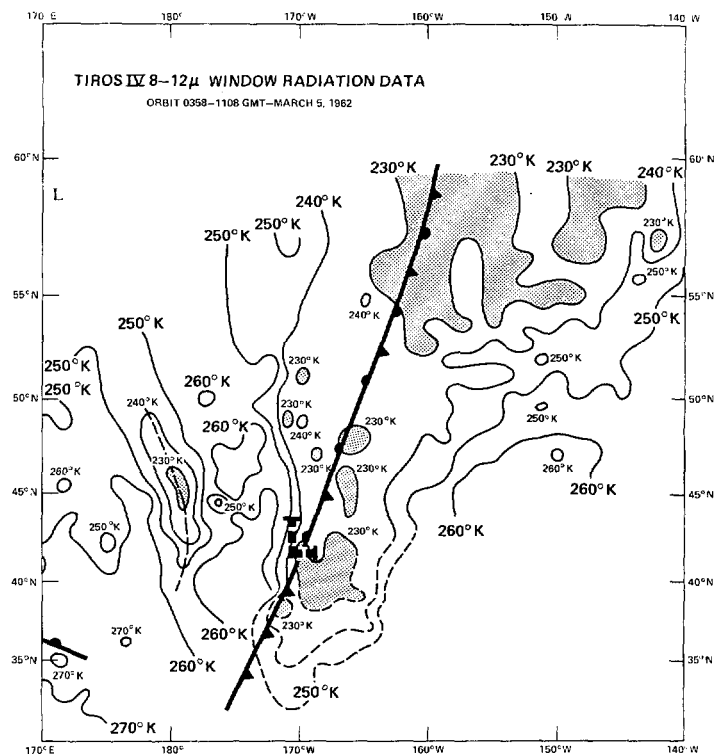


FIGURE 3.—TIROS IV window radiation data for Mar. 5, 1962 (orbit 358); dashed lines show data added from orbit 357.

weakening of the frontal band.

Figures 7–14 depict the window radiation grid print maps and surface weather charts that were coincident

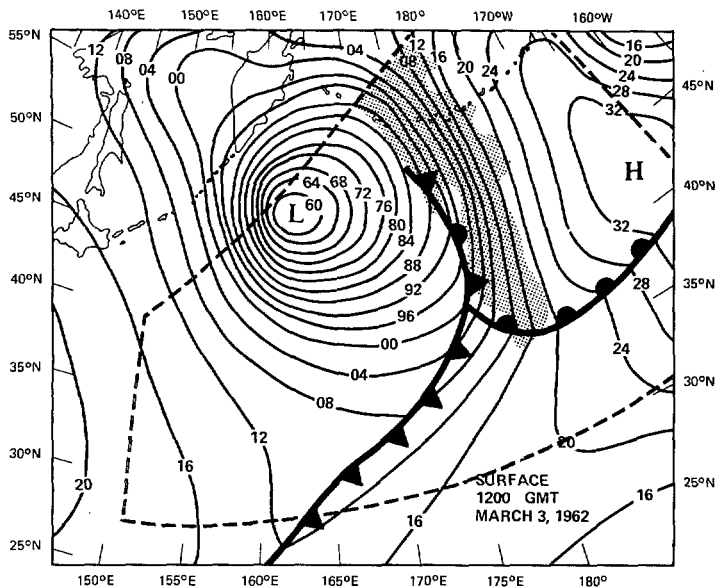


FIGURE 4.—Surface chart for 1200 GMT on Mar. 3, 1962; the swath of the radiation data is outlined, and the stippled area is where the equivalent blackbody temperatures were $\leq 230^\circ\text{K}$.

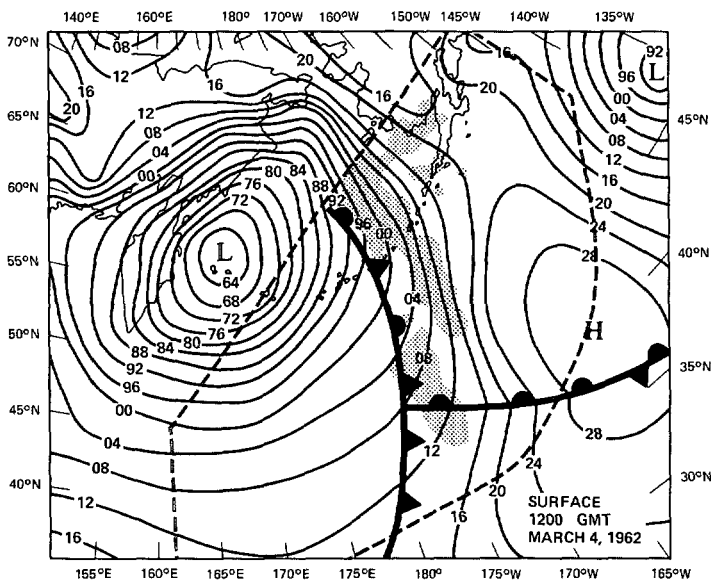


FIGURE 5.—Same as figure 4, except for 1200 GMT on Mar. 4, 1962.

with a rapidly developing secondary cyclone in the eastern Pacific. The energetic new system developed suddenly near the base of the occlusion of an old and filling occluded cyclone of moderate intensity. The cloud top heights associated with the old primary cyclone were lower (as measured by increased equivalent blackbody temperatures) in the region north and east of the base of the occlusion between 1000 GMT on March 19 and 0900 GMT on March 20 (figs. 7 and 8), although the central pressure of the storm did not change (figs. 10 and 11). The apparent decrease in cloud heights is shown by the almost total absence of equivalent blackbody temperatures $\leq 230^\circ\text{K}$ to the east and north of the base of the occlusion in figure 8. In fact, some equivalent blackbody temperatures $\geq 250^\circ\text{K}$ occurred within that region. Thus, while it was not noticeable on the surface chart, the cloud

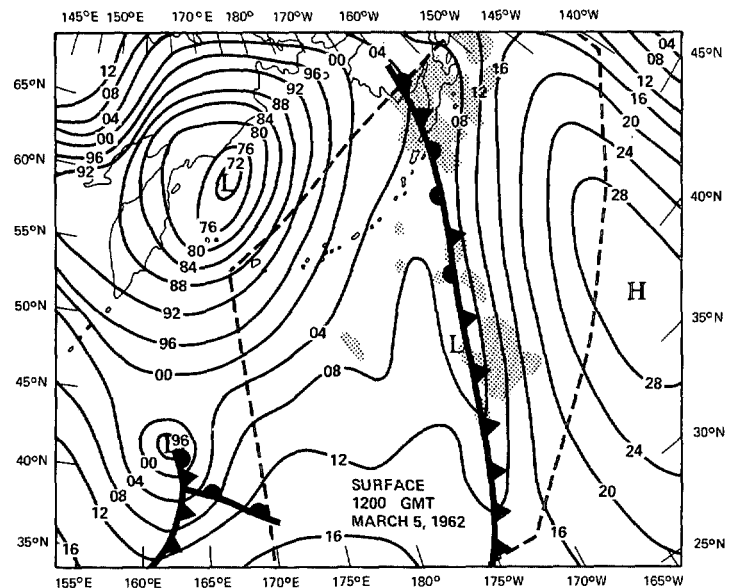


FIGURE 6.—Same as figure 4, except for 1200 GMT on Mar. 5, 1962.

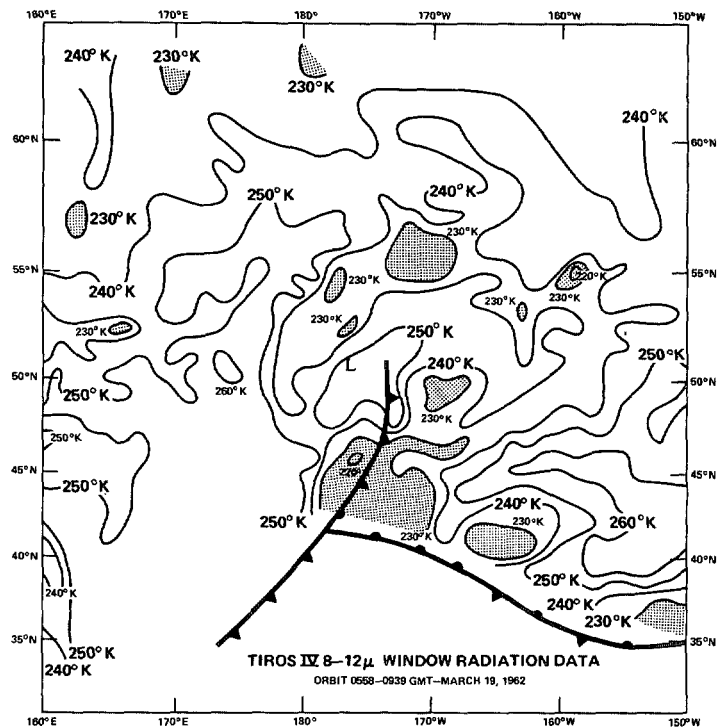


FIGURE 7.—TIROS IV window radiation data for Mar. 19, 1962 (orbit 558).

pattern associated with the primary storm had undergone some deterioration. By 0600 GMT on March 21, the primary system had weakened and had continued to move steadily east-northeastward (fig. 12). There was no strong evidence of a secondary development in the surface analysis. The only possible hint was a 25-kt west-northwest surface wind reported by a ship some 400 n.mi. south-southeast of the occluded cyclone center. This flow compares with a west-southwest flow of similar strength relative to the storm center some 18 hr earlier. The greater northerly component indicates that some low-level "digging" is starting to take place to the rear of the front. This evi-

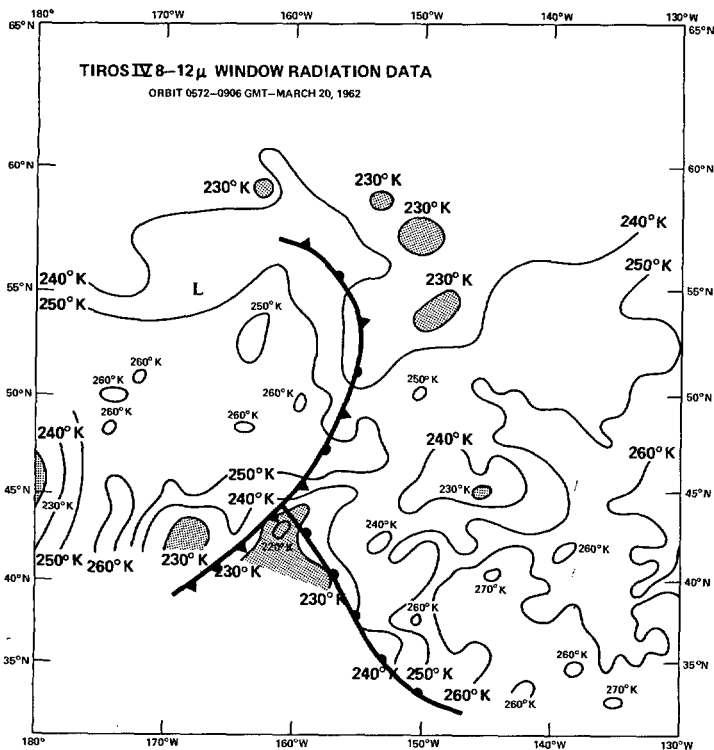


FIGURE 8.—TIROS IV window radiation data for Mar. 20, 1962 (orbit 572).

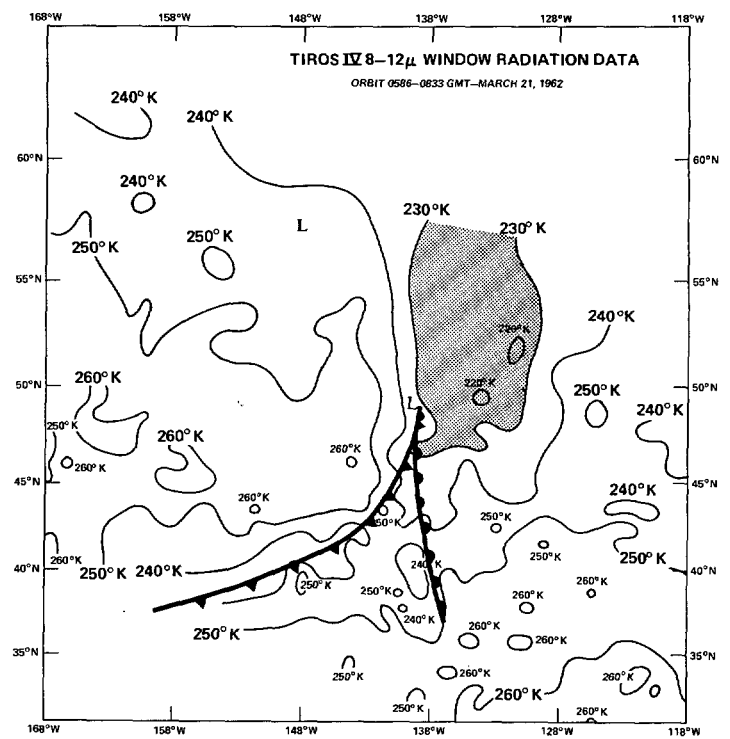


FIGURE 9.—TIROS IV window radiation data for Mar. 21, 1962 (orbit 586).

dence, although of interest, would almost certainly be insufficient to indicate an imminent surface development. A glance at the equivalent blackbody temperature field for 0900 GMT shows that sweeping changes had occurred in 24 hr (fig. 9). Instead of a rather disorganized cloud pattern east and north of the base of the occlusion, the equivalent blackbody temperature field indicates an area of solid high clouds over an extensive area. These high clouds probably reflect a dynamical trend toward stronger upward motions. Shenk (1963) showed that the strongest upward motions were associated with the lowest equivalent blackbody temperatures.

Tremendous changes began to occur on the surface charts within a few hours following the observation of the dramatic change in the cloud pattern. By 1200 GMT on March 21 (fig. 13), strong evidence was present that a new circulation was developing to the southeast of the old primary cyclone. Twelve hours later, the rapidly deepening and intensifying secondary cyclone was located not far from the west coast of the United States, and high winds were occurring along the coastline (fig. 14). The new system deepened some 16 mb between 1200 GMT on March 21 and 0000 GMT on March 22. Thus, the strong trend toward lower equivalent blackbody temperatures between 0900 GMT on March 20 and 0900 GMT on March 21 had been coincident with a rapidly deepening secondary development.

A history similar to that observed on the surface charts occurred at 500 mb. Between 1200 GMT on March 19 and 0000 GMT on March 21, a shortwave trough advanced through the central Pacific. It gradually weakened and was not detectable on the 0000 GMT March 21 chart. Twelve

hours later, a moderately strong shortwave trough was analyzed at about 140°–150° W. Very strong cold advection on the upstream side of the trough line suggested continued digging and deepening of the trough. Thus by 1200 GMT on March 21, it was evident from the analysis of the conventional data that a new cyclone was forming and that the potential existed for the development to continue. Undoubtedly, some cloud development had occurred before the TIROS pass (0900 GMT). This development, perhaps less striking than what is shown, would have been useful in indicating the presence of favorable conditions for secondary development before it was reasonably certain that such development would occur from examining the available conventional data.

The above discussions suggest that, when a reversal occurs in the gradual increase of the equivalent blackbody temperatures associated with the weakening frontal cloud band of an existing cyclone, the probability of secondary cyclone development has increased. Figure 15 is a schematic drawing of an old occluded system, and the dashed region represents one likely area where this temperature reversal might occur. The temperature-reversal hypothesis was more quantitatively examined by computing the mean and frequency distributions of the equivalent blackbody temperatures within this dashed region for all four cases. This axis of the rectangle was always oriented north-south. As can be seen in figure 15, the dashed area is determined by the position of the base of the occlusion which cannot always be located precisely over the oceans. However, this area is large, and thus the precise location was not judged to be a critical factor. After the formation of a secondary cyclone, the lower left corner of the area was located at the

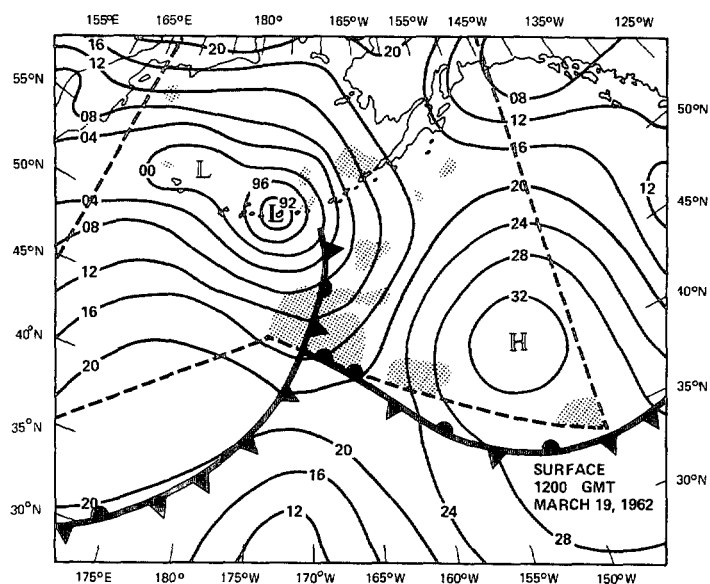


FIGURE 10.—Surface chart for 1200 GMT on Mar. 19, 1962; the swath of the radiation data is outlined, and the stippled area is where the equivalent blackbody temperatures were $\leq 230^\circ\text{K}$.

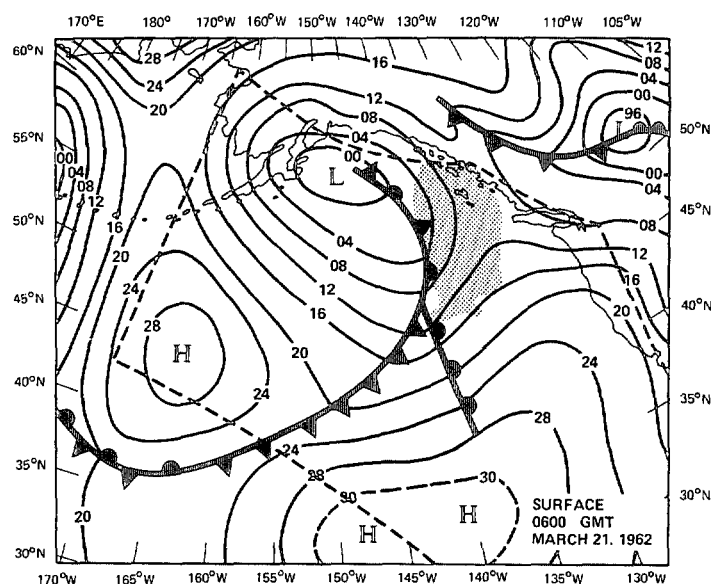


FIGURE 12.—Same as figure 10, except for 0600 GMT on Mar. 21, 1962.

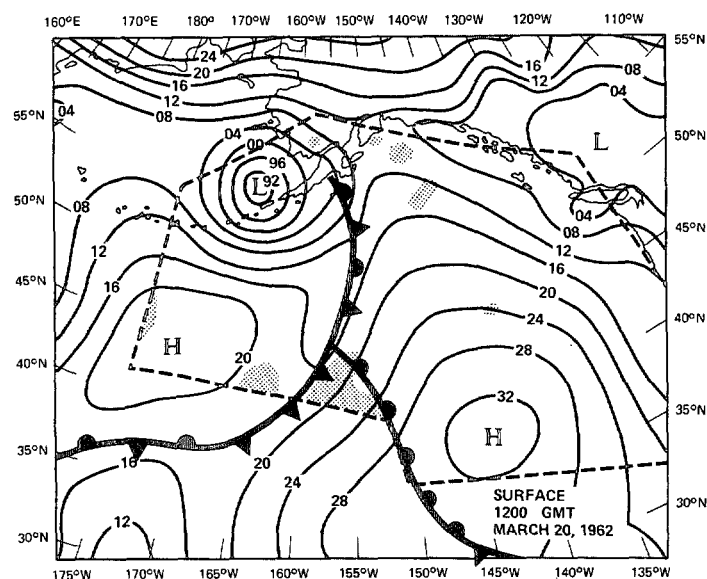


FIGURE 11.— Same as figure 10, except for 1200 GMT on Mar. 20, 1962.

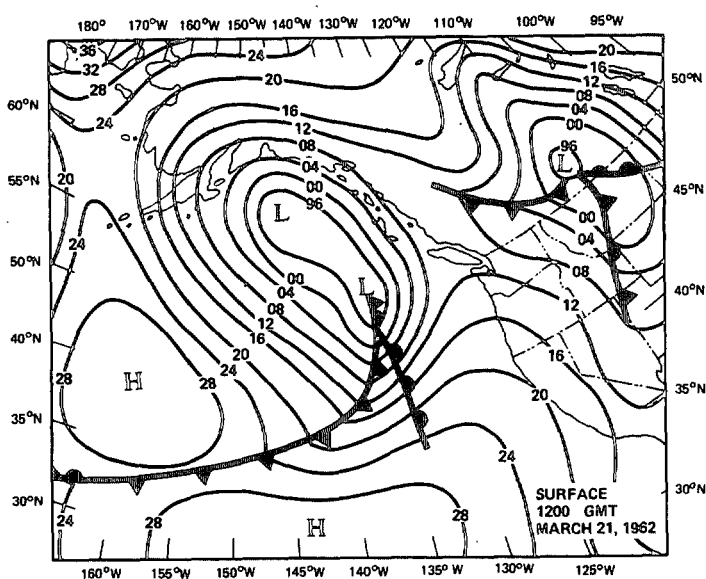


FIGURE 13.—Surface chart for 1200 GMT on Mar. 21, 1962.

secondary cyclone center. Table 2 presents the frequency distribution of equivalent blackbody temperatures within the dashed area, with class intervals of 10°K . The average equivalent blackbody temperatures were computed by assigning the values within the class to the central values of the class, except for the class of $\leq 220^\circ\text{K}$ where all values were assigned an equivalent blackbody temperature of 220°K . In the two cases where no substantial secondary development occurred at the base of the occlusion, a gradual day-to-day increase in the average equivalent blackbody temperature was noted within the dashed region. Also, there is a day-to-day decrease in the number of

equivalent blackbody temperature measurements in the $221^\circ\text{K} \leq 230^\circ\text{K}$ class. The average day-to-day increase in equivalent blackbody temperature within the dashed region was 4°K when no substantial secondary development occurred.

Table 2 shows that before the development of the March 21 secondary cyclone (case 3), there was a sharp rise (13.6°K) in the average equivalent blackbody temperature in the dashed area (1000 GMT on March 19 to 0900 GMT on March 20). This was followed by the even more dramatic decrease of 23.6°K in equivalent blackbody temperature in the next period. A decrease in equivalent blackbody temperatures within the dashed region also occurred with the other case of secondary development,

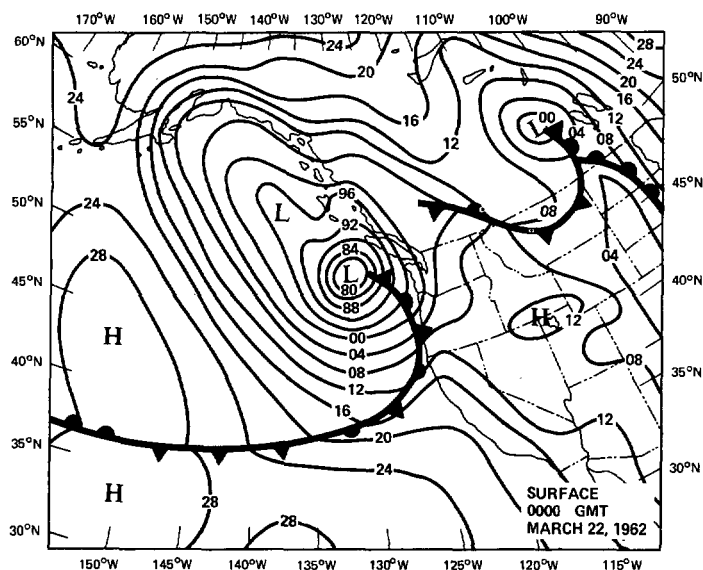
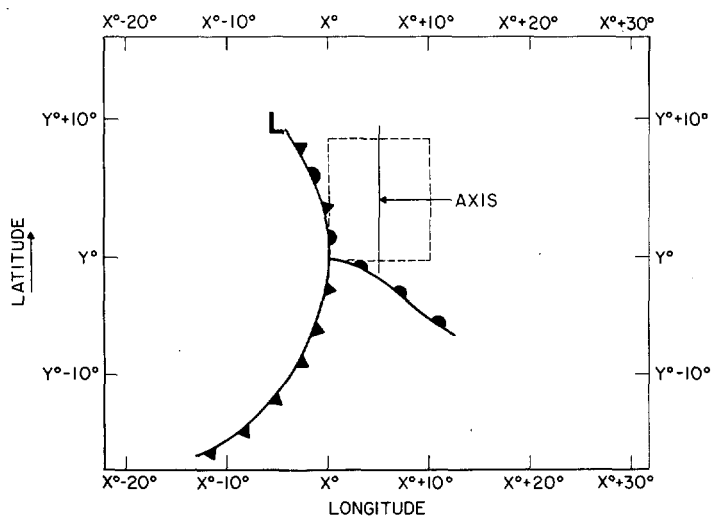


FIGURE 14.—Surface chart for 0000 GMT on Mar. 22, 1962.

FIGURE 15.—Schematic diagram of the frontal structure of an occluded cyclone; the dashed region is oriented north-south with the lower left corner at the triple point (latitude y° , longitude x°).

although the decrease was less (6.5°K). Therefore, when secondary cyclone generation was noted, the average equivalent blackbody temperature decrease was 15°K .

The decreases in the average equivalent blackbody temperature within the dashed region in figure 15 for the two secondary cyclone development situations probably reflect an increase in upward vertical motion over the dashed region. The initiation of the strong upward motion is most likely associated with positive vorticity advection over the dashed area, which is a major contributor to surface cyclogenesis (Petterssen 1956). For the March 21 secondary development, the 24-hr decrease in average equivalent blackbody temperature (23.6°K) over the dashed region would be coincident with a 4-km rise in the

TABLE 2.—Frequency of TIROS IV window radiation measurements within 10°K class limits for each case within the dashed region shown in figure 15

Equivalent black-body temperatures ($^\circ\text{K}$)	Date and principal orbit no.		
	Case 1		
	Mar. 3, 1962 (330)	Mar. 4, 1962 (344)	Mar. 5, 1962 (358)
220	0	0	0
221 ≤ 230	42	37	13
231 ≤ 240	18	24	47
241 ≤ 250	6	8	10
251 ≤ 260	6	3	2
Average	231.7°K	231.8°K	235.1°K
	Case 2		
	Mar. 16, 1962 (515)		Mar. 17, 1962 (529)
220	0		0
221 ≤ 230	10		0
231 ≤ 240	10		0
241 ≤ 250	15		6
251 ≤ 260	20		40
261 ≤ 270	17		24
271 ≤ 280	0		2
Average	248.3°K		258.1°K
	Case 3		
	Mar. 19, 1962 (558)	Mar. 20, 1962 (572)	Mar. 21, 1962 (586)
220	1	0	2
221 ≤ 230	36	0	58
231 ≤ 240	18	9	12
241 ≤ 250	7	39	0
251 ≤ 260	10	24	0
Average	233.5°K	247.1°K	223.5°K
	Case 4		
	Mar. 21, 1962 (585)		Mar. 22, 1962 (598)
220	0		1
221 ≤ 230	8		33
231 ≤ 240	36		14
241 ≤ 250	16		9
251 ≤ 260	12		6
Average	239.4°K		232.9°K

cloud top heights if the cloud tops existing at the beginning of the period were simply lifted at an average rate of 4.5 cm sec^{-1} during the interval. More likely, the clouds present at the end of the period were formed at least in part from air parcels lifted from some level above the cloud tops that existed at the beginning of the period.

4. CONCLUSIONS

These four case studies indicate that, when a secondary cyclone is beginning to form at the surface near the base of the occlusion, a substantial day-to-day decrease in the equivalent blackbody temperature has already occurred in an area within a few hundred miles to the northeast of the center of the new circulation. No equivalent blackbody temperature decrease was noted within the same area when no new development or a very weak stable wave developed. The equivalent blackbody temperature decrease was greatest for the case where the secondary cyclone developed most rapidly. This result suggests that the rapidity of surface development may be related to the

rate of change of equivalent blackbody temperature within the frontal cloud band that is related to the upward vertical motions reflected by the positive vorticity advection.

The onset of cloud development relative to surface development should be examined more closely. This might be possible with the receipt of infrared measurements in the fall, winter, or spring seasons at 12-hr intervals from a polar-orbiting satellite. Even better cloud-surface development relationships should be possible as soon as radiometers are placed in geosynchronous orbit when observations will be made at intervals of less than an hour. In addition to better temporal resolution, current or planned sensors placed in these orbits will have better thermal and spatial resolutions than were possible with the earlier satellites. The improved resolutions should afford a better definition of the cloud surface and hence permit a deeper probing into this type of meteorological phenomena.

REFERENCES

- Anderson, R. K., Ferguson, E. W., and Oliver, V. J., "The Use of Satellite Pictures in Weather Analysis and Forecasting," *WMO Technical Note No. 75*, World Meteorological Organization, Geneva, 1966, 184 pp.
- Boucher, Roland J., Bowley, C. J., Merritt, E. S., Rogers, C. W. C., Sherr, Paul E., and Widger, W. K., Jr., "Synoptic Interpretations of Cloud Vortex Patterns as Observed by Meteorological Satellites," *Final Report*, Contract No. Cwb-10630, Aracon Geophysics Co., Concord, Mass., Nov. 1963, 194 pp.
- Goddard Space Flight Center, NASA, *TIROS IV Radiation Data Catalog and Users' Manual*, Aeronomy and Meteorology Division, National Aeronautics and Space Administration, Greenbelt, Md., Dec. 15, 1963, 250 pp.
- Petterssen, Sverre, *Weather Analysis and Forecasting*, 2d edition, Vol. 1, McGraw-Hill Book Co., Inc., New York, 1956, 428 pp.
- Shenk, William E., "TIROS II Window Radiation and Large Scale Vertical Motion," *Journal of Applied Meteorology*, Vol. 2, No. 6, Dec. 1963, pp. 770-775.
- Shenk, William E., "Meteorological Satellite Views of Cloud Growth Associated With the Development of Secondary Cyclones," *NASA Technical Note No. D-5680*, National Aeronautics and Space Administration, Washington, D.C., Apr. 1970, 24 pp.
- Sherr, Paul E., and Rogers, C.W.C., "The Identification and Interpretation of Cloud Vortices Using TIROS Infrared Observation," *Final Report*, Contract No. Cwb-10812, Aracon Geophysics Co., Concord, Mass., Mar. 1965, 77 pp. plus appendix.

[Received January 26, 1970; revised June 5, 1970]